

# A laser heating method for estimating the thermal balance of burning solid propellants

Akira Kakami<sup>\*†</sup>, Shota Terashita<sup>\*</sup>, and Takeshi Tachibana<sup>\*</sup>

<sup>\*</sup>Department of Mechanical Engineering, Kyushu Institute of Technology 1-1 Sensui-cho, Tobata, Kitakyushu 804-8550, JAPAN  
TEL : +81-93-884-3163 FAX : +81-93-884-3163

<sup>†</sup>Corresponding address : kakami@mech.kyutech.ac.jp

Received : July 13, 2009 Accepted : September 15, 2009

## Abstract

This paper proposes a method to apply laser heating to solid propellant combustion in order to evaluate the heat feedback rate from flame to burning surface,  $H_f$ . A burning surface was irradiated with a laser in a pressure-regulated test chamber. From a simple heat balance model on the burning surface, the burning rate was dependent on the laser power density, and the values of  $H_f$  were determined using the dependence. HTPB/AP based solid propellant samples were irradiated at laser power densities ranging from 0.3 to 0.8 W mm<sup>-2</sup>. The experiments showed that the burning rate increased with the laser power density and that  $H_f$  values were successfully evaluated and were almost monotonously augmented with back pressure and ranged from 1.0 to 2.0 W mm<sup>-2</sup>.

**Keywords** : Solid propellant, Combustion, Heat feedback rate, Laser

## Nomenclature

$\lambda_p$	= thermal conductivity of solid propellant, W/m K
$T$	= temperature, K
$r$	= burning rate, m/s
$x$	= moving coordinate whose origin is fixed at burning surface, m
$\rho_p$	= mass density of solid propellant, kg m <sup>-3</sup>
$Q$	= heat of reaction, kJ/kg
$I_L$	= laser power density on burning surface of solid propellant, W m <sup>-2</sup>
$\Lambda_p$	= heat flux supplied from burning surface to solid phase of propellant, W m <sup>-2</sup>
$H_f$	= heat feedback rate from the flame to burning surface, W m <sup>-2</sup>
$(dT/dx)_{s+}$	= gas-phase temperature gradients in the vicinity of burning surface, W m <sup>-2</sup>
$r\rho_p Q_s$	= heat intensity of reaction on the burning surface, W m <sup>-2</sup>
$C_p$	= specific heat of solid propellant, J/kg K
Subscripts	
0	= initial condition
s	= burning surface
p	= solid phase propellant

$g$  = gas phase

## 1. Introduction

We propose to apply laser heating to solid propellant combustion for the estimation of the heat feedback rate from flame to burning surface,  $H_f$ . Conventionally, temperature distribution in both solid and gas phase is measured with thermocouples embedded in a regressing solid propellant<sup>(1-3)</sup>, the temperature distribution measurement yielding the values of  $H_f$ . In this method, however, the thermocouples should have a diameter as small as 10  $\mu$ m to have sufficiently low thermodynamic time constants, and should be strenuously embedded in the solid. The thermocouples are damaged or melted by the flame and consequently are difficult to reuse. Additionally, the thermal conductivity in the gas phase, which would be varied with its temperature and pressure, was necessary for the calculation of  $H_f$ .

In this study, we propose a non-intrusive method using laser heating for the evaluation of  $H_f$  without measuring or estimating the gas-phase thermal conductivity. A combustion chamber with a laser-introducing window was designed and used to show the feasibility of the proposed method. Hydroxyl Terminated Poly Butadiene / Ammo-

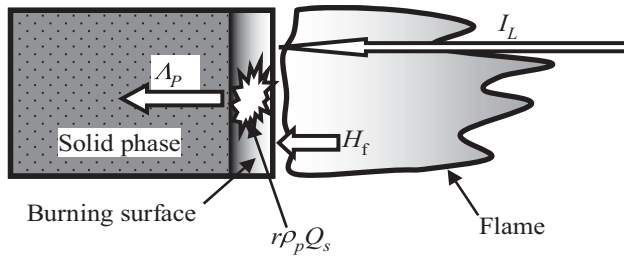


Fig. 1 Heatbalance of burning solid propellant.

niium Perchlorate (HTPB/AP) composite samples were tested in the combustion chamber at absolute pressures from 0.03 to 0.3 MPa. The heat feedback from the flame to the burning surface was estimated from the dependence of burning rates on laser power density with the proposed method that will be mentioned below.

## 2. Principle of Method

Figure 1 shows a schematic of the heat balance in a burning solid propellant under laser irradiation. A heat balance equation in the burning surface has been proposed to analyze the combustion of the solid propellant<sup>4,5</sup>. The model treats heat transfer in the solid phase as follows: heat transfer from burning surface to solid phase,  $\Lambda_s$ , heat production on burning surface,  $r\rho Q_s$  and heat feedback from flame to burning surface,  $H_f$ . In the proposed method, the burning surface is heated with a laser, and by applying a new laser heating term,  $I_L$ , the heat balance equation is expressed as

$$\Lambda_p = \rho_p r Q_s + H_f + I_L \quad (1)$$

In the solid phase, the steady-state heat transfer equation using the coordinate  $x$  with its origin taken at the burning surface is expressed as

$$\lambda_p \frac{d^2 T}{dx^2} - \rho_p C_p r \frac{dT}{dx} = 0 \quad (2)$$

With the boundary conditions:

$$\begin{aligned} T &= T_s \quad \text{at } x = 0 \\ T &= T_0 \quad \text{at } x = -\infty \end{aligned}$$

Integrating Eq. (2) with  $x$ , the heat flux from the burning surface to the solid phase  $\Lambda_p$  is expressed by

$$\Lambda_p = \lambda_p \left( \frac{dT}{dx} \right) = C_p \rho_p r (T_s - T_0) \quad (3)$$

Substituting Eq. (3) to Eq. (1) yields

$$r = a_L I_L + b_L \quad (4)$$

where

$$a_L = \frac{1}{C_p \rho_p (T_s - T_0) - \rho_p Q_s} \quad (5)$$

$$b_L = \frac{H_f}{C_p \rho_p (T_s - T_0) - \rho_p Q_s} \quad (6)$$

From Eqs. (5) and (6), the heat feedback rate to the burning surface,  $H_f$ , appears as the equation:

$$H_f = \frac{b_L}{a_L} \quad (7)$$

The value of  $H_f$  is determined by substituting the experimentally evaluated values of  $a_L$  and  $b_L$  into Eq. (7).

## 3. Experimental apparatus

### 3.1 Test chamber

Figure 2 shows a schematic diagram of the experimental apparatus. The test chamber is cylindrical with an outer diameter of 120 mm, an inner diameter of 54 mm and a length of 320 mm. The solid propellant samples were fixed with a sample holder, which is clasped in the left end. On the other end, the test chamber had a 50-mm-diam BK-7 laser-introducing window with anti-reflection coating. On both sides of the test chamber, 50-mm-diam BK-7 windows were also placed for observing the combustion.

This test chamber has gas inlet ports for introducing nitrogen purge gas and outlet ports for expelling nitrogen and exhaust. The nitrogen purge gas was provided from a high pressure cylinder through the gas inlet ports and was divided into two streams in the test chamber. One of the streams was supplied into the sample holder and went through an array of holes to let the nitrogen stream flow along the sample.

The other nitrogen gas stream was injected to the laser-introducing window in order to prevent the burned particles from adhering to the window surface and to remove the plume from the laser-beam path toward the sample. The nitrogen flow rate for the laser-introducing window, which went toward the burning surface, would disturb the combustion. Hence, the mass flow was set as sufficient not to disturb the combustion.

The exhaust gas went out of the combustion chamber by itself at back pressures above 0.1 MPa and was evacuated by a rotary pump through a cubic surge tank 320 mm at back pressures below 0.1 MPa. During the experiments, the back pressure was regulated by adjusting the inlet port and outlet port valves. The back pressure of the test chamber was variable from 0.3 kPa to 0.3 MPa.

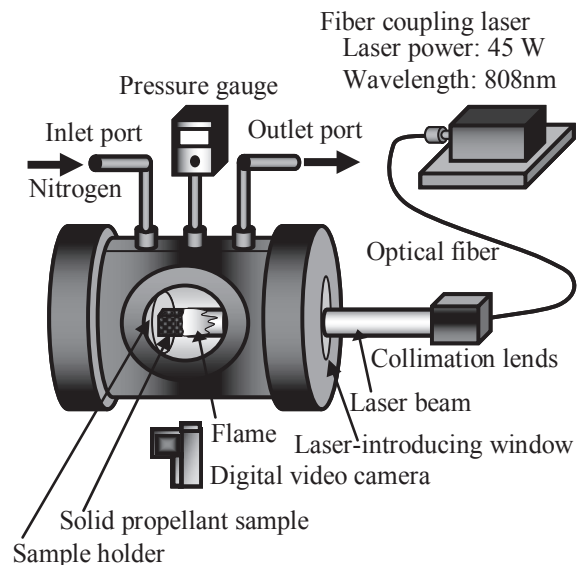


Fig. 2 Experimental apparatus.

### 3.2 Laser

A continuous-wave fiber-coupling laser diode (JOLD-45-CPXF-1L 808 0.4P, JENOPTIC Laserdiode GmbH) was utilized as a heat source to the burning surface. The laser has a wavelength of 808 nm and a rated laser power of 45 W. In order to stabilize the laser power, the temperature of the laser diode was regulated using a Peltier device to keep it at 23–26°C. The laser was driven with a constant current power source, and the laser power was adjusted from 10 to 45 W with the driving current.

The laser beam was introduced through an optical fiber of 400  $\mu\text{m}$  core diameter to an optical collimation lens unit (FCC-A, LIMO-Lissotschenko Mikrooptik GmbH). The laser beam was collimated by the unit and then had a divergent angle of 40 mrad and a diameter of approximately 10 mm.

The collimated laser beam was guided to the test chamber through the laser-introducing window in such way that the solid propellant sample inside the test chamber was aligned with the laser beam. The window was coated with an anti-reflection layer on its surfaces with a transmission ratio of more than 99.5 %.

Figure 3 shows a typical laser power density distribution in the neighborhood of the laser-irradiated burning surface. This profile was obtained by scanning the laser beam using an optical fiber with a core diameter of 100  $\mu\text{m}$ . One end of the optical fiber was exposed to the laser beam and was moved horizontally and vertically using two linear stages. The laser beam was transmitted to a NIST-traceable photodiode optical sensor (S140A, Thorlabs). The output voltage of the optical sensor was recorded by an IBM-PC compatible computer through a data acquisition interface board (PCI-3521, Interface Corp.). The sample used in the experiments had a burning surface of 2 mm  $\times$  2 mm in section. In the burning surface, the laser profile was quite uniform with an average laser power density of 0.65  $\text{W mm}^{-2}$  and a standard deviation of  $2.3 \times 10^{-2} \text{ W mm}^{-2}$ . The laser power density provided to the burning surface of the sample ranged from 0.30 to 0.80

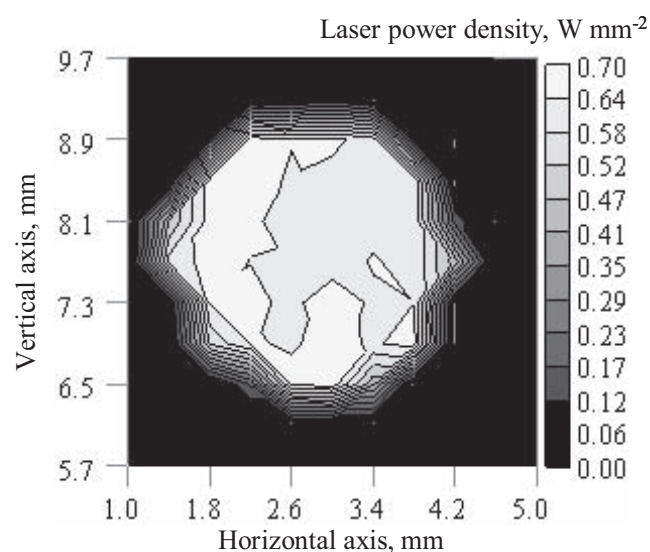


Fig. 3 Atypical laser density distribution in the region near solid propellant surface.

Table 1 Ingredients and weight mixture ratios of test solid propellants (Sample #1 is non-self burning, #2 is self-burning)

Sample	HTPB	AP	Carbon black	Aluminum
#1	30	70	0.5	
#2	20	80		20

$\text{W mm}^{-2}$ .

### 3.3 Solid propellant samples

Table 1 displays the composition of the samples used in the experiment. The samples were HTPB/AP composite solid propellants with an average AP diameter of approximately 5  $\mu\text{m}$ . Extra ingredients such as carbon black and aluminum powder were added to augment laser beam absorption.

Sample #1 is a non-self combustible solid propellant whose combustion is sustained by heating the burning surface with an external heat source and is terminated by interrupting the heat supply. Our previous study has shown that the combustion of sample #1 is controllable with laser heating up to 0.09 MPa<sup>3</sup>. In the case of sample #1, the laser diode is a heat source for both controlling combustion and investigating  $H_f$ . On the other hand, sample #2 is a self-combustible solid propellant, which autonomously keeps burning without laser heating of the burning surface once ignited, in which case the laser is a heat source for estimating  $H_f$ .

The solid samples were typically 2 mm  $\times$  2 mm  $\times$  15 mm rectangular bars. The size of the cross section was determined from the laser power density distribution shown in Fig. 3. Owing to this shape, the standard deviation in laser power density on the burning surface was 3.5 % of the average.

### 3.4 Burning rate measurement

The flame and solid sample regression was recorded at a frame rate of 30 Hz by a digital CCD video camera from a lateral view, as shown in Fig. 2. Burning rates were evaluated from the images. A personal computer captured sequential images from the digital CCD video camera and calculated the burning surface position on each frame using brightness distribution along the longitudinal axis of the solid sample. The burning rates were determined with the least square method from the time variation in burning surface position.

## 4. Results and Discussion

### 4.1 Non self-combustible solid propellant

Figure 4 illustrates a typical image of the regressing burning solid propellant in the experiment when sample #1 was irradiated with a beam 0.8  $\text{W mm}^{-2}$  in laser power density. The preferable alignment of the laser beam with the solid sample and the uniform laser power density allowed the burning surface to maintain regress well along the longitudinal axis of the solid sample. This propellant could not support the combustion by itself, and hence, the

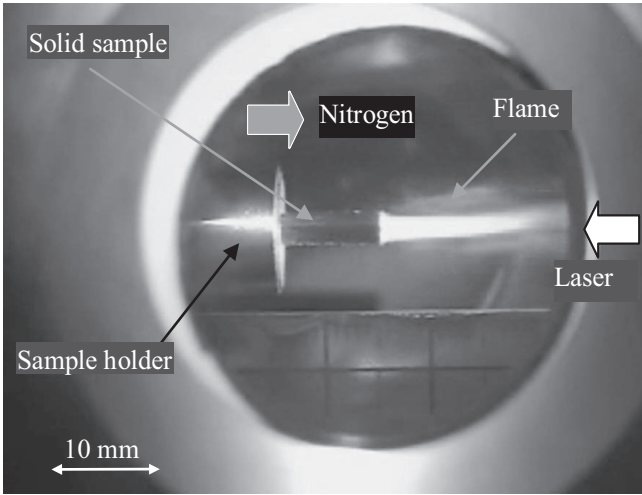


Fig. 4 Image of burning solid sample under laser heating. Laser power density:  $0.7 \text{ W mm}^{-2}$ , backpressure:  $0.2 \text{ MPa}$ , sample #1.

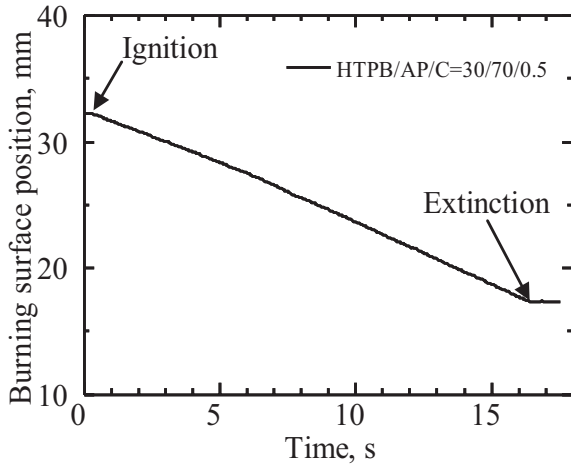


Fig. 5 Burning surface regression with time.

combustion was terminated by interrupting laser irradiation to the solid propellant. The time variation in the burning surface position was evaluated using sequential images such as Fig. 4 and is exhibited in Fig. 5. The solid samples yielded constant burning rates during the laser heating in all experiments. Hence, the burning rates measured in the experiment can be used for the estimation of  $H_f$  values using Eq. (7).

The variation in burning rate with back pressure was shown in Fig. 6. With the entire laser power density tested, the burning rate increased monotonously with back pressure until  $0.18 \text{ MPa}$ . On the other hand, the burning rate was abated with back pressure at pressures over  $0.22 \text{ MPa}$ , and the combustion became unstable. The flame repetitively expanded and shrunk during the laser irradiation.

Figure 7 shows the dependence of the burning rate on the laser power density. Fitting the burning rates to Eq. (4) by the least square method gives the coefficients  $a_L$  and  $b_L$  with the determination  $R^2$ , which are listed in Table 2. All the values of  $R^2$  were over  $0.90$  with the exception of the case at  $0.22 \text{ MPa}$ , and then the burning rate linearly increased with the laser power density. Hence, experimen-

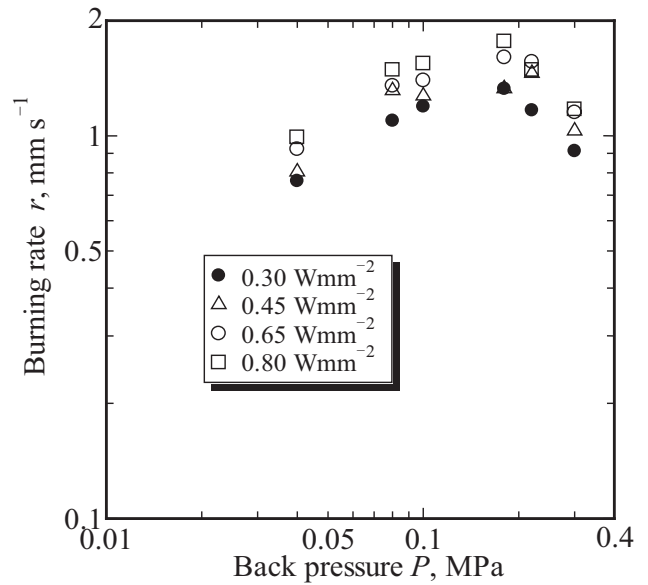


Fig. 6 Variation in burning rate with back pressure on back pressure for sample #1.

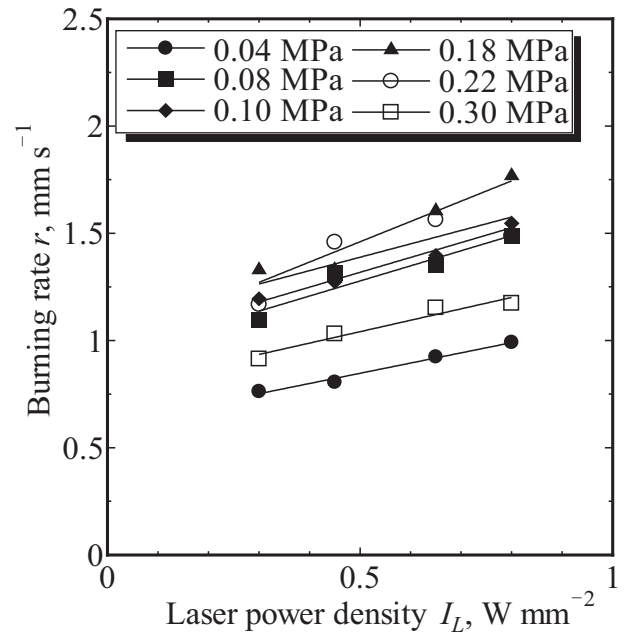


Fig. 7 Dependence of the burning rate  $r$  on the laser power density  $I_L$  with laser power density for sample #1 under different pressures.

tally evaluated values of  $a_L$  and  $b_L$  yield  $H_f$  values using Eq. (7), because the burning rate  $r$  remained constant during laser irradiation as shown in Fig. 5 and the determination  $R^2$  was as high as  $0.9$  where the relation between burning rate  $r$  and laser power density was fitted using Eq. (4).

Figure 8 represents the variation in  $H_f$  with back pressure for sample #1. The errors were evaluated using the determination  $R^2$  listed in Table 2. At  $0.22 \text{ MPa}$ , the error of  $H_f$  is large in comparison with the other back pressures. This would be attributed to the unstable combustion at this pressure.

#### 4.2 Self-burning solid propellant

For sample #2, the combustion was stably sustained during the laser irradiation and in contrast with sample #

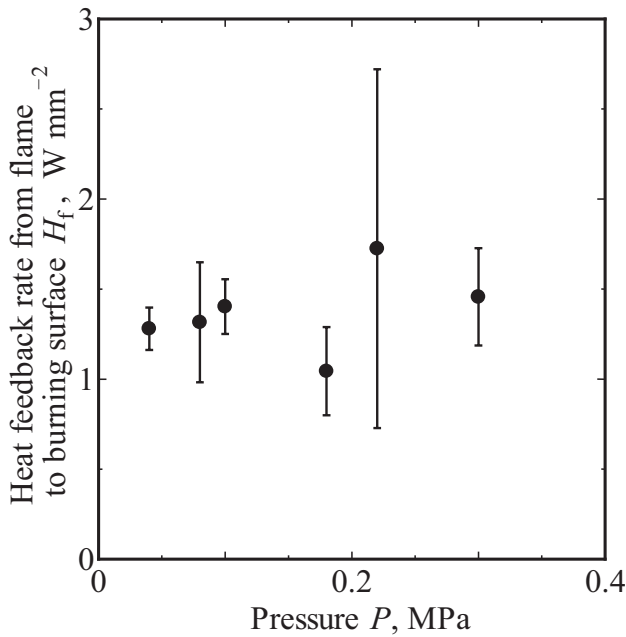


Fig.8 Evaluated variation in heatfeedback from flame to burning surface with back pressure for sample #1.

Table 2 Evaluated  $a_L$  and  $b_L$  obtained from the experiment for non-self burning sample #1

Pressure $P$ , MPa	$a_L$	$b_L$	$R^2$
0.04	0.48	0.61	0.99
0.08	0.70	0.93	0.90
0.10	0.69	0.97	0.98
0.18	0.95	0.99	0.92
0.22	0.62	1.1	0.63
0.30	0.53	0.78	0.94

1, even after interrupting the laser heating. During the combustion, neither flickering nor extinguishing occurred at any back pressure tested in the experiment. The time variation in the position of the regressing burning surface, which was similar with that of sample#1 shown in Fig. 5, shows that the burning rate was constant even with self-burning solid propellants in laser assisted combustion. Hence, the combustion of sample #2 met one of the necessary conditions for estimating  $H_f$  using Eq. (7). Figure 9 illustrates the burning rate variation with back pressure. The burning rate increased monotonously with back pressure with the laser irradiation.

The burning rate of self-burning propellants was also monotonously augmented with laser power density, as shown in Fig. 10. Fitting the burning rates and laser power density with Eq. (4) yields the values of  $a_L$ ,  $b_L$  and  $R^2$  listed in Table 3. The evaluated coefficients of determination,  $R^2$  showed that the burning rates linearly increased with laser power density even for the self-combustible solid propellant. Hence, the linear dependence of the burning rate on the laser power density yields the values of  $H_f$  with relatively smaller errors using Eq. (7). Figure 11 shows that the variation in  $H_f$  with back pressure. The values of  $H_f$  somewhat increased with back pressure and ranged from 1.0 to 2.0  $W\ mm^{-2}$ .

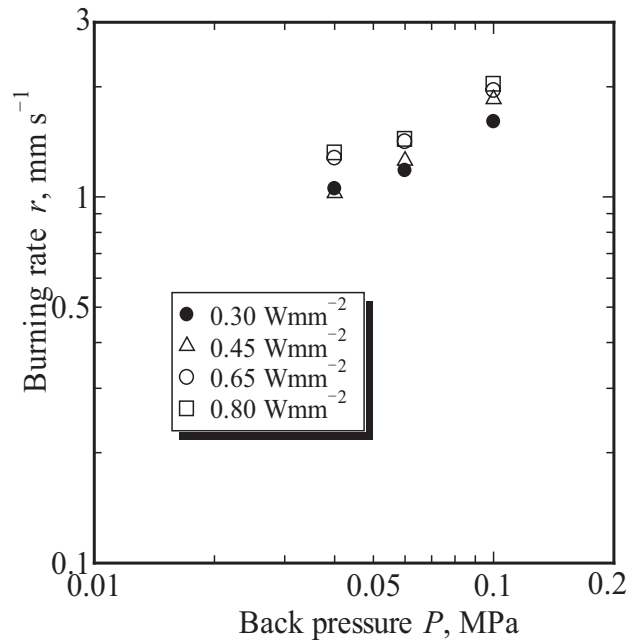


Fig.9 Dependence of burning rate  $r$  on back pressure  $P$  for sample #2 with each laserpower densities  $I_L$ .

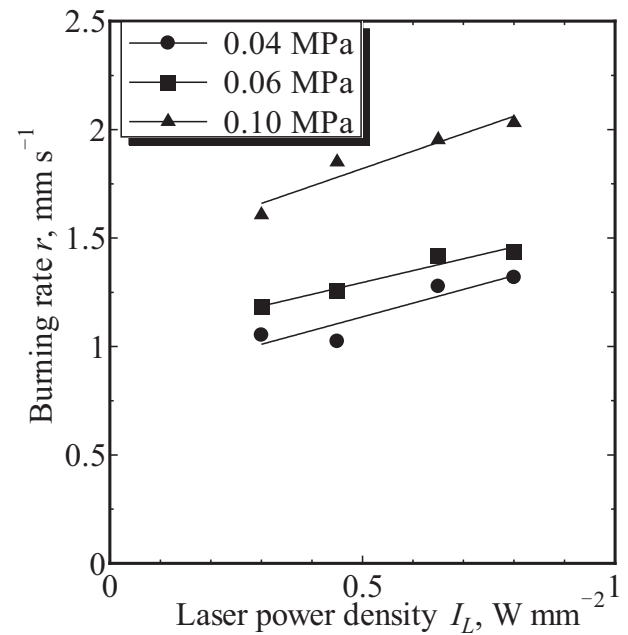


Fig.10 Variation in burning rate  $r$  with laser power density  $I_L$  for sample #2 at backpressures ranging 0.04 to 0.10 MPa.

### 4.3 Comparison with thermocouple measurement

For the purpose of validating the proposed method, the  $H_f$  values for a self-combustible HTPB/AP solid propellant were estimated using empirical data shown in Ref.6. The thermocouple measurement yielded the fitted curve of the gas-phase temperature gradient in the vicinity of the burning surface  $(dT/dx)_{s+}$  for the HTPB/AP=16/84 propellant, as shown in Fig. 12<sup>5)</sup>. The gas-phase thermal conductivity in the vicinity of burning surface,  $\lambda_{s+}$  was obtained using with Chemical Equilibrium Application (CEA)<sup>6)</sup>. In the calculation, the gas-phase temperature near burning surface is assumed to be 600 K, which was measured at back pressures ranging from 0.02 to 0.1 MPa<sup>5)</sup>. The product of  $\lambda_{s+}$  and  $(dT/dx)_{s+}$  provides the heat

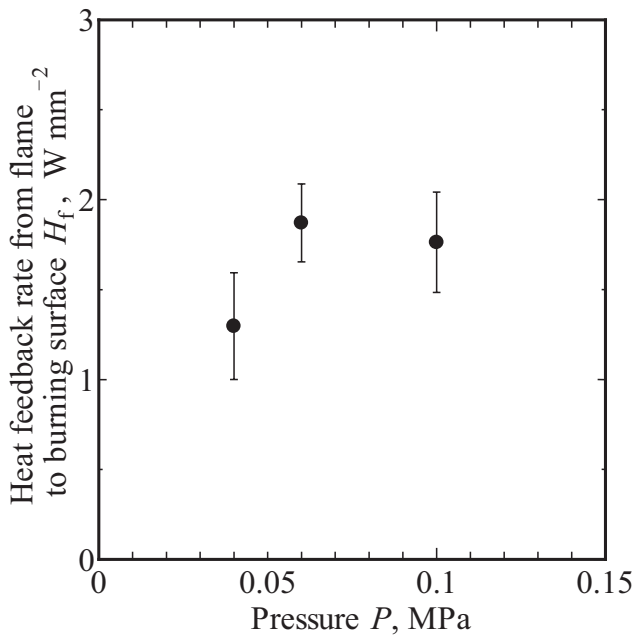


Fig.11 Evaluated variation in heatfeedback from flame to burning  $H_f$  surface with back pressure for sample #2.

Table 3 Evaluated  $a_L$  and  $b_L$  obtained from the experiment for self burning sample #2

Pressure $P$ MPa	$a_L$	$b_L$	$R^2$
0.04	0.63	0.82	0.92
0.06	0.55	1.0	0.98
0.10	0.80	1.4	0.96

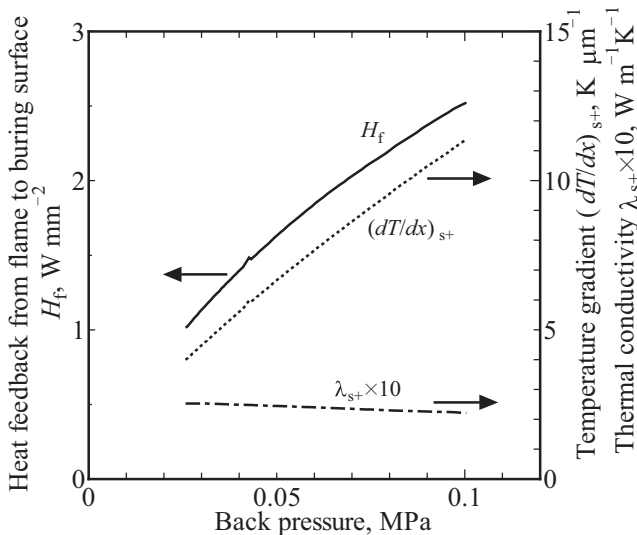


Fig.12 Evaluated heat feedback from flame to burning surface for HTPB/AP=16/86 propellant using CEA and reference 6.

feedback from flame to burning surface, which are illustrated as the solid line in Fig. 12. The values of  $H_f$  for HTPB/AP=14/86 monotonously increased from 1.0 to 2.4  $W\ mm^{-2}$  with back pressure. For samples #1 and #2, the proposed method showed that the  $H_f$  almost monotonously increased with pressure below 0.1 MPa and varied from 1.0 to 2.0  $W\ mm^{-2}$ , as shown in Figs. 8 and 11. From these results, the proposed method would be reasonable for the

evaluation of  $H_f$ .

### 5. Summary

This paper proposes a new method for rating the heat feedback from flame to burning surface  $H_f$  for solid propellants, and is summarized as follows :

1. Laser heating to the burning surface was applied for the non-intrusive estimation of  $H_f$  using the dependence of the burning rate on laser power density. This method requires no gas-phase thermal conductivity, which would be obtained with chemical equilibrium calculation.
2. In both self-sustained and non self-combustible solid samples, the burning rates kept constant during laser irradiation and were almost linear with laser power density. Consequently, the burning rates under laser irradiation were applicable to the estimation of the heat feedback from flame to burning surface.
3. The  $H_f$  values evaluated with the proposed method almost monotonously increased with back pressure and were coincident with the estimated values using thermocouple-yielded temperature gradients and gas-phase thermal conductivity provided with chemical equilibrium calculation.

### Acknowledgments

This work was partially supported by a Grant-in-Aid for Scientific Research (B) No.17360411 by the Japan Society for the Promotion of Science (JSPS). The authors also acknowledge Asahi Kasei Chemicals Corporation for the sample supply.

### References

- 1) G. P. Sutton and O. Biblarz, "Rocket Propulsion Elements, 7<sup>th</sup> ed.", Chaps. 11 and 14 (2000) Wiley-Interscience.
- 2) T. Tachibana and H. Ohisa, J. of Propulsion and Power, 15, 6 (1999).
- 3) A. Kakami, R. Hiyamizu, K. Shuzenji and T. Tachibana, J. of Propulsion and Power, 24, 6 (2008).
- 4) L. De Luca, W. E. Price and M. Summerfield, (ed.), "Non-steady Burning and Combustion Stability of Solid Propellants", Chaps. 7 and 14 (1992), American Institute of Aeronautics and Astronautics, Inc.
- 5) N. Kubota, "Propellants and Explosives 2nd Edition", Chap. 7 (2007), Wiley-VCH Verlag GmbH & Co. KGaA.
- 6) NASA Glenn Research Center, Chemical Equilibrium with Applications (CEA), available at <http://www.grc.nasa.gov/WWW/CEAWeb/>.

# 固体推進薬燃焼の熱バランス算出に資する レーザー加熱法の提案

各務 聡<sup>\*†</sup>, 寺下祥太<sup>\*\*</sup>, 橘 武史<sup>\*</sup>

本論文では、固体推進薬燃焼における火炎から燃焼面への熱のフィードバック量 ( $H_f$ ) を評価するためにレーザー加熱を適用することを提案する。本方式では、圧力を一定に保った燃焼容器に固体推進薬を入れ燃焼面にレーザーを照射し、燃焼速度とレーザーパワー密度との関係から  $H_f$  を算出するのである。HTPB/AP系固体推進薬をサンプルとしてレーザーパワー密度を  $0.3\sim 0.8 \text{ W mm}^{-2}$  の範囲で変化させたところ、燃焼速度はレーザーパワー密度に依存し  $H_f$  を算出するに至った。 $H_f$  は背圧と共にほぼ単調に増加しその範囲は  $1.0\sim 2.0 \text{ W mm}^{-2}$  であった。

\*九州工業大学工学研究院機械知能工学研究系宇宙工学部門 〒804-8550 福岡県北九州市戸畑区仙水町1-1

\*\*九州工業大学工学部機械知能工学科 〒804-8550 福岡県北九州市戸畑区仙水町1-1  
TEL: 093-884-3163 FAX: 093-884-3163

†Corresponding address: kakami@mech.kyutech.ac.jp